

Journal Pre-proof

Visible-light assisted of nano Ni/g-C₃N₄ with efficient photocatalytic activity and stability for selective aerobic C–H activation and epoxidation

Mona Hosseini-Sarvari , Zahra Akrami

PII: S0022-328X(20)30452-6
DOI: <https://doi.org/10.1016/j.jorganchem.2020.121549>
Reference: JOM 121549



To appear in: *Journal of Organometallic Chemistry*

Received date: 11 July 2020
Revised date: 5 September 2020
Accepted date: 27 September 2020

Please cite this article as: Mona Hosseini-Sarvari , Zahra Akrami , Visible-light assisted of nano Ni/g-C₃N₄ with efficient photocatalytic activity and stability for selective aerobic C–H activation and epoxidation, *Journal of Organometallic Chemistry* (2020), doi: <https://doi.org/10.1016/j.jorganchem.2020.121549>

This is a PDF file of an article that has undergone enhancements after acceptance, such as the addition of a cover page and metadata, and formatting for readability, but it is not yet the definitive version of record. This version will undergo additional copyediting, typesetting and review before it is published in its final form, but we are providing this version to give early visibility of the article. Please note that, during the production process, errors may be discovered which could affect the content, and all legal disclaimers that apply to the journal pertain.

© 2020 Published by Elsevier B.V.

Highlights

- A procedure for the performance of a metal-organic catalyst with high photocatalytic activity is described.
- Ligand-free nano Ni/g-C₃N₄ was synthesized by using the photodeposition procedure.
- Ligand-free nano Ni/g-C₃N₄ exhibited high photocatalytic performance in the selective aerobic C–H activation and epoxidation.
- The high yields of products, economical, environmentally friendly, and simple procedures are the advantages of the method.

Journal Pre-proof

Visible-light assisted of nano Ni/g-C₃N₄ with efficient photocatalytic activity and stability for selective aerobic C–H activation and epoxidation

Mona Hosseini-Sarvari*, Zahra Akrami

Department of Chemistry, Faculty of Science, Shiraz University, Shiraz, 7194684795 I.R. Iran. E-mail: hossaini@shirazu.ac.ir

Abstract

A selective, economical, and ecological protocol has been described for the oxidation of methyl arenes and their analogs to the corresponding carbonyl compounds and epoxidation reactions of alkenes with molecular oxygen (O₂) or air as a green oxygen source, under mild reaction conditions. The nano Ni/g-C₃N₄ exhibited high photocatalytic activity, stability, and selectivity in the C–H activation of methyl arenes, methylene arenes, and epoxidation of various alkenes under visible-light irradiation without the use of an oxidizing agent and under base free conditions.

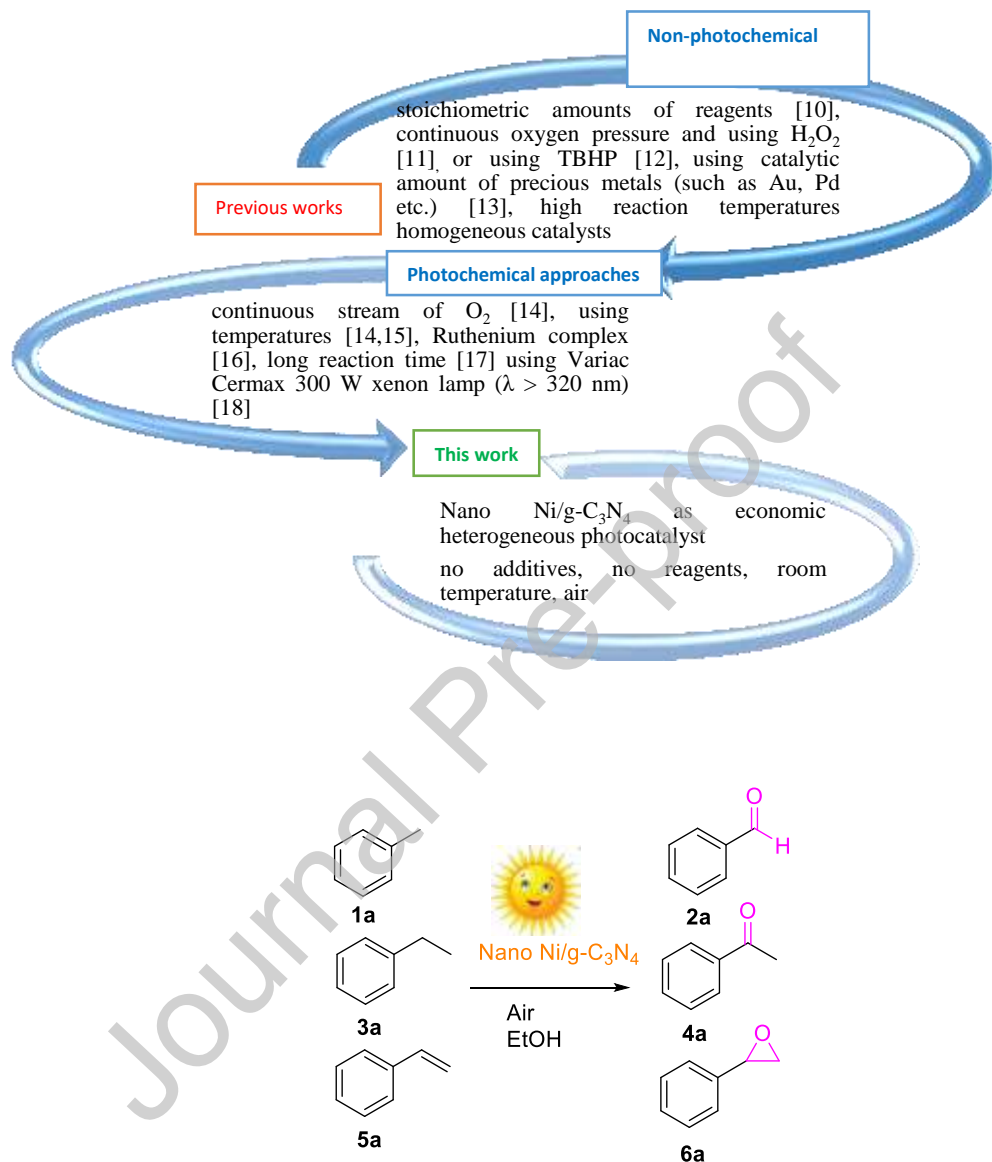
Keywords

C-H activation; Epoxidation; Nano Ni/g-C₃N₄; Photocatalyst; Visible light

1. Introduction

The one-pot addition of molecular oxygen as a “green” oxidant into hydrocarbons (alkanes and alkenes) to obtain a family of aldehydes, ketones, and epoxy derivatives is an extremely desirable reaction. So a lot of attention has been paid to the search for novel raw materials for the chemical industry including drugs, polymers, agricultural and synthetic materials [1]. Oxygen, particularly if received from the air, demonstrates the perfect oxidant even more efficiently than the commonly mild oxidant “hydrogen peroxide” [2]. Besides, O₂ has a wide range of derivatives while retaining high selectivity, reduced environmental impact, and high atom economy [3]. Besides, if molecular oxygen can be actuated at room temperatures under standard pressure condition it will be the most appropriate oxidizing agent. So photocatalytic processes can be applied for selective and greener oxidation by O₂ as the oxidant [4]. The selective oxidation of methyl arenes and the oxidation of benzylic (C-sp³) hydrocarbons to the analogous carbonyl groups is a key reaction in chemical synthesis [5,6]. Likewise, styrene epoxidation reactions show a vital part in industrial processes. Styrene oxide is usually synthesized directly by epoxidation of alkenes with peroxy acids or by chlorohydrin processes which are highly-cost, low-yield of epoxide, and leads to serious environmental contamination [7]. Most of these reactions have tough

conditions that are briefly mentioned in the Scheme 1. As a result, we have decided to apply an efficient technique in organic synthesis [8,9] for avoiding the disadvantages of current protocols for the oxidative C–H activation.



Scheme 1. The synthesis of aldehyde, ketone, and epoxide derivatives in previous reports and this work

Natural Photosynthesis is a model for the development of non-natural photoredox systems by utilizing several semiconductor photocatalysts [19]. Nowadays heterogeneous photocatalytic based on the use of noble metal-semiconductor hybrid nanoparticles are used for new organic synthesis and many other uses [20]. Among all reported photocatalysts g-C₃N₄ (a semiconductor)

has attracted extensive attention [21-24]. The g-C₃N₄ owns a graphitic piling of C₃N₄ layers, that are created from fused tris-triazine cycles by tertiary amines, lead to its heptazine units and a high density [25,26]. As a result of the sp² hybridization of nitrogen and carbon atoms that form π -conjugated graphitic systems, g-C₃N₄ is so remarkable as a visible light absorption range of 450–460 nm with an optical band gap of 2.7 eV [27]. Thermal and chemical stability, numerous interesting electric properties, non-toxicity, low cost, and easy to get from abundant sources of organic nitrogen like melamine and urea are unique features of g-C₃N₄ [28]. These polymers possess efficient transportation and separation of electron-hole pairs which causes photoactivity [29]. But despite these benefits doping cocatalyst on the g-C₃N₄ nanosheets is a highly desired method as the electron-hole recombination rate is high in pure g-C₃N₄ and surface area photocatalytic activity is quite low [30]. Metal doping has several advantages such as: accelerating the separation and transfer of charge, enhancing the visible-light absorption, lowering the bandgap, and prolonging the charge carriers' lifetime for g-C₃N₄, that all of these features are required for the efficient photocatalytic process [31]. Ni is abundant, cheap, good stability, and is also high activity metal. In the presence of nickel, the separation of electron-hole pairs can be done successfully, arising from the alteration of the surface band bending which can be faster surface reaction rates and can suppress back reactions, which results in good photocatalytic performance in contrast to the pure g-C₃N₄ [32]. So, loading Ni on the g-C₃N₄ is an efficient strategy and we understood that the nano Ni/g-C₃N₄ photocatalyst is an applicable choice for the oxidative C–H activation, and leads to the selective oxidation and preparation of organic structures containing oxygen (Scheme 1).

2. Experimental

2.1. Materials

Total chemicals were either provided in our laboratories or were gained from Fluka, Aldrich, and Merck. All the solvents dried in agreement with standard procedures.

2.2 Analysis methods

The proceeds of the reactions were controlled by thin-layer chromatography (TLC) employing silica gel SILG/UV 254 plates. Column chromatography was run on minor columns of silica gel. IR spectra of the samples were registered on a Shimadzu FTIR-8300 spectrophotometer by KBr pellets. The amount of nickel nano Ni/g-C₃N₄ was assessed using inductively coupled plasma (ICP). Power X-ray diffraction analysis (XRD) was measure with Cu K α (λ = 1.54178 Å) irradiation. The distribution morphology of the nano Ni/g-C₃N₄ was established by applying scanning electron microscopy (SEM). The specific surface

areas (SSABET; (m² /g)) of the nanopowders were identified with the nitrogen adsorption measurement utilizing the BET procedure at 77 K (BELsorp-mini II). Shimadzu UV-2450 spectrophotometer was carried out the UV–vis diffuse reflectance spectrum. Melting points were measured by Buchi Melting Point B-545 electrical melting point equipment. ¹H NMR and ¹³C NMR spectra were registered in CDCl₃ as solvent using Bruker, Avance 400 (operating at 400 MHz for ¹H and 100 MHz for ¹³C), with TMS as an internal standard (multiplicity: s = singlet, d= doublet, t = triplet, dd = doublet of doublets, m = multiplet). The lamps applied for photochemical reactions were 12 W white, blue, red LED and 11 W green LED. A blue LUX* plus (made from china) LED A 65 with a voltage of 220- 240 V, frequency of 50/60 Hz, lumens 1150 lm, and a power of 12 watts was used.

2.3. Preparation of g-C₃N₄

The g-C₃N₄ was prepared according to the procedure reported by Li [33]. A Coors high-alumina crucible was charged with 10 g of melamine powder, next placed in a 673in³ muffle furnace (115V / 14 Amps) at a heating rate of 20° C /min to 500° C in 2h. In the following for formation better structure, it was put at 520° C for 2 h.

2.4. Preparation of nano Ni/g-C₃N₄

The nano Ni/g-C₃N₄ was prepared by an altered photodeposition procedure [34]. 10 mg g-C₃N₄, 3 mL triethanolamine (TEOA), 250 μL NiCl₂ (0.1 M) solution, 2 mL NaH₂PO₂ (0.1 M) aqueous solution, and 4.9 mL H₂O were blended in a round bottom flask at room temperature. The system was stirred for 40 min under nitrogen atmosphere. Then, the mixed solution was irradiated under UV-vis light (300 W Xe lamp) for 30 min. The final point involved washing collected precipitates with distilled water to dispel the residues of reactants.

2.5. General procedure for C–H activation reactions

A mixture of toluene (1 mmol) in EtOH (2 mL)) placed in 10 mL round bottom flask, nano Ni/g-C₃N₄ (6wt%, 0.01 g) was added and the set of the reaction was illuminated by 12 W blue LED Lamp at a distance 3 cm. Generally, optimized conditions were maintained (air atmosphere and room temperature). The completion of the reaction was specified by thin-layer chromatography. After centrifuging and separating the photocatalyst, 12 mL ethyl acetate diluted the mixture of reactions. The pure product was obtained through silica gel column chromatography of crude mixture (petroleum ether/ethyl acetate).

2.6. General procedure for epoxidation reactions

A mixture of styrene (1 mmol) in CH₃CN (2 mL)) placed in 10 mL round bottom flask, nano Ni/g-C₃N₄ (6 wt%, 0.012 g) was added and the set of the reaction was illuminated by 12 W blue LED Lamp at a distance 3 cm. Generally, optimized conditions were maintained (air atmosphere and room temperature). The completion of the reaction was specified by thin-layer chromatography. After centrifuging and separating the photocatalyst, 12 mL ethyl acetate diluted the mixture of reactions. The pure product was obtained through silica gel column chromatography of crude mixture (petroleum ether/ethyl acetate).

3. Results and discussion

3.1. Mechanism

We have used this photocatalyst to deliver a selective oxidation of benzylic (C- sp³) hydrocarbons and epoxidation of alkenes in the presence of O₂ or air. With this in mind, we questioned whether selective oxidation might be possible using the O₂ in combination with photoredox and nickel catalysis. In this photocatalytic reaction system, O₂⁻ played a significant role. The photocatalytic mechanism of this oxidation reaction can involve two main stapes: 1) formation of activated oxygen by nano Ni/g-C₃N₄; 2) selective oxidation of C-C and C=C bonds, therefore a plausible conclusive photocatalytic mechanism is outlined in Figure 1. Upon exposure g-C₃N₄, to visible light, the holes begot in its VB by transferred electrons from VB of g-C₃N₄ to CB. Additionally, the doping of metallic Ni on g-C₃N₄ displays the role of co-catalysts can boost its VB level. In comparison to the potential of CB, g-C₃N₄ composites (around -1.1 vs Ag/AgCl, at pH=7) the potential of metallic Ni (-1.0 V vs Ag/AgCl, at pH=7) more negative. Thus Nickel-metal takes the photo-generated electrons from g-C₃N₄, which leads to the enhancement of charge disassociation and improved activity [35] As a result, it causes better oxidation on the g-C₃N₄ surface. Thus, activated oxygen (O₂⁻) will be generated via grabbing electrons of Ni by O₂. Subsequently, a single-electron transfer to the hole obtained in the g-C₃N₄ nanoparticles oxidizes the substrate to the intended radical cation. The activated oxygen species selectively oxidize the cationic radicals (a) and (b), leading to the formation of benzaldehyde or olefin oxides via rearrangement or splitting of a cyclic peroxide intermediate. Therefore, we began our investigation into the photooxidative hydrocarbons and epoxidation alkenes by preparing nano Ni/g-C₃N₄. In this route, Ni(II) is reduced to Ni(0) by photogenerated electrons and was doped on the electron external surface of g-C₃N₄. (with particle size ~5-9 nm).

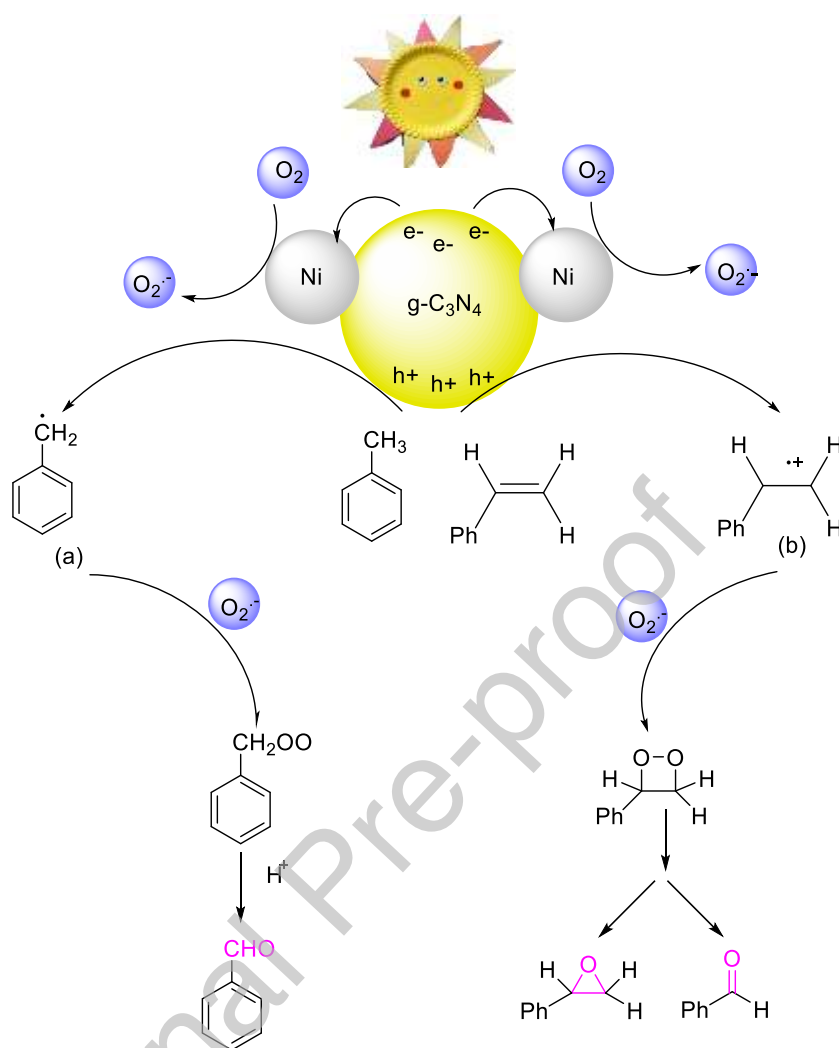


Figure 1. Proposed mechanism for the photocatalytic oxidation and epoxidation reaction.

3.2. Catalyst characterization

With this proposed mechanism in mind, first, the catalyst was prepared and then the characterization was performed by energy-dispersive X-ray spectroscopy (EDX), powder X-ray diffraction (XRD), SEM, transmission electron microscopy (TEM), BET, and UV-visible analysis. The optical absorption of non-modified $g\text{-C}_3\text{N}_4$ and Ni-6 wt% $g\text{-C}_3\text{N}_4$ was characterized by UV-vis diffuse reflectance spectroscopy. As remarked in Figure 2, with Ni-loading in $g\text{-C}_3\text{N}_4$ support, the absorption peak of modified $g\text{-C}_3\text{N}_4$ progressively switches to the longer wavelength region. The optical band gaps are 2.76 and 2.38 for $g\text{-C}_3\text{N}_4$ and nano Ni/ $g\text{-C}_3\text{N}_4$, respectively. Decreasing the bandgap after loading Ni implies a high level of interaction between Ni species and $g\text{-C}_3\text{N}_4$ support. Also the stronger visible light absorption than non-modified $g\text{-C}_3\text{N}_4$, in fine accord with their color shift of the compounds (Figure 2).

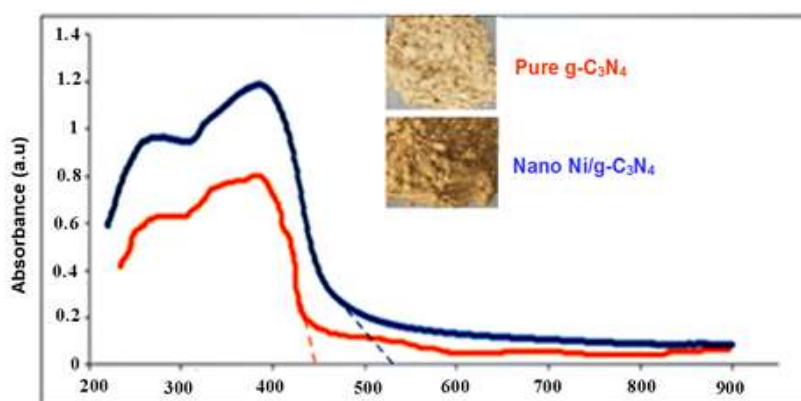


Figure 2. UV-vis absorption spectra of g-C₃N₄ and nano Ni/g-C₃N₄.

Figure 3 shows the XRD patterns of pure g-C₃N₄ and nano Ni/g-C₃N₄ (6 wt%) nanoparticles. The minor signal at 13.08, conforming to the interplanar length that is related to interlayer packing. The sharper signal at 27.41 is a distinctive interlayer amassing peak of graphitic systems. Pure g-C₃N₄ and Ni supported on g-C₃N₄ represented distinguished signal at 27.41, it indexed that the structural characteristics of g-C₃N₄ were reserved well in the process doping of nickel. For its part, the pure g-C₃N₄ signal intensity decreased slightly with the doping of the Ni, which showed that the surface of g-C₃N₄ was loaded by Ni. Also, the weakening and broadening of this peak proposed Ni on the surface of g-C₃N₄ slightly prevented the diffraction of crystallinity of g-C₃N₄ [34]. It can be regarded that for Ni supported on g-C₃N₄, new signals at $2\theta = 44.5^\circ$, 51.8° , and 76.4° become visible respectively, in proportion to (111), (200), and (220) crystal planes of Ni, which indicates compliance with the standard sheets of metallic Ni (JCPDS 87-0712) (Fig 3). The average particle sizes of the unmodified and nano Ni/g-C₃N₄, calculated by the Scherrer's formula, are around 4.6 nm.

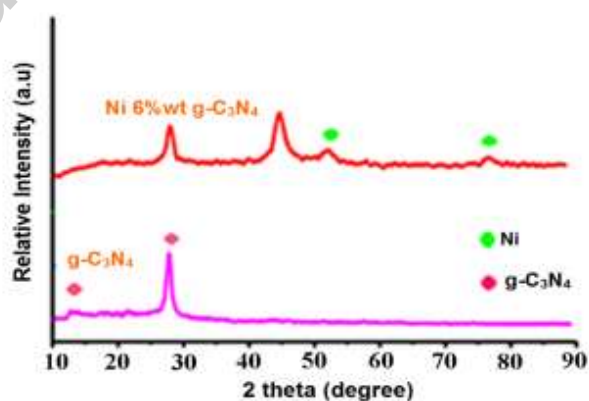


Figure 3. XRD pattern of g-C₃N₄ and nano Ni/g-C₃N₄ at room temperature.

EDX analysis revealed the presence of nickel. Meanwhile, the P element was not displayed in the evaluation data of energy disperse X-ray, which indicated that no phosphorus compounds were created on the surface of pure $g\text{-C}_3\text{N}_4$ (Figure 4). Also, the induced coupled plasma (ICP) analysis confirmed that the nano $\text{Ni/g-C}_3\text{N}_4$ contains only 6 wt % Ni.

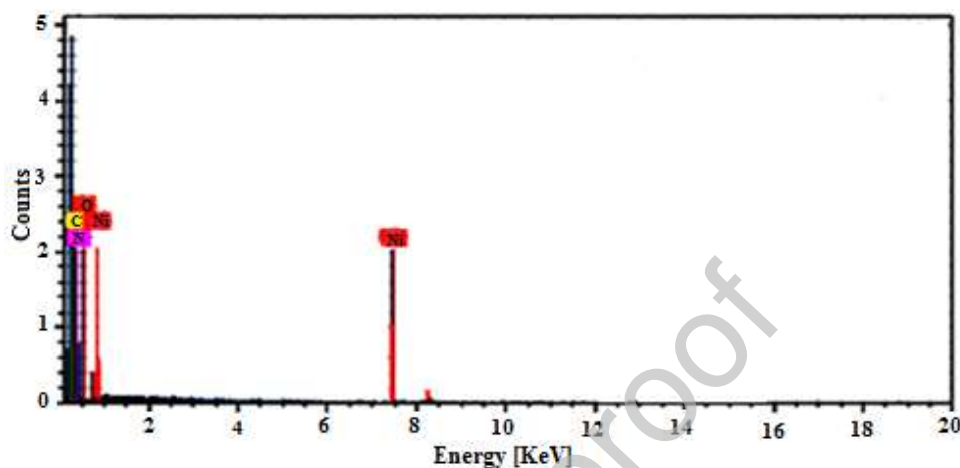


Figure 4. EDX spectrum of nano $\text{Ni/g-C}_3\text{N}_4$.

The scanning electron microscopy (SEM) image of freshly prepared nano $\text{Ni/g-C}_3\text{N}_4$ appears in Figure 5. The nano $\text{Ni/g-C}_3\text{N}_4$ with a diameter of nearly 10–20 nm and also mixed cubic and spherical morphology can be noted. Cubic morphology increases the absorption in the visible light range [36].

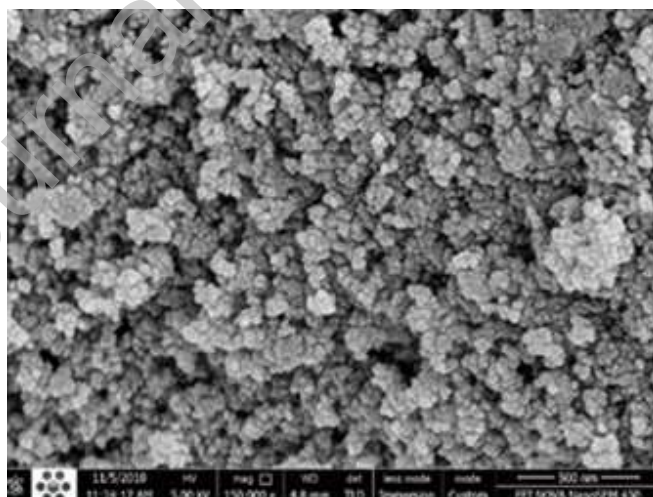


Figure 5. SEM images of nano $\text{Ni/g-C}_3\text{N}_4$

Similarly, Figure 6 is followed by a transmission electron microscopy (TEM) image of the synthesized nano $\text{Ni/g-C}_3\text{N}_4$. We could determine that Ni is coated conveniently by $g\text{-C}_3\text{N}_4$ with cube and sphere form

and the range of size obtained from TEM is roughly between 5-9 nm which affirms the data in the XRD pattern. The ratio of surface /sub-surface defects can be elevated to allow charge-carrier separation to increase which is achieved with the sub-10 nm size of the particle [37].

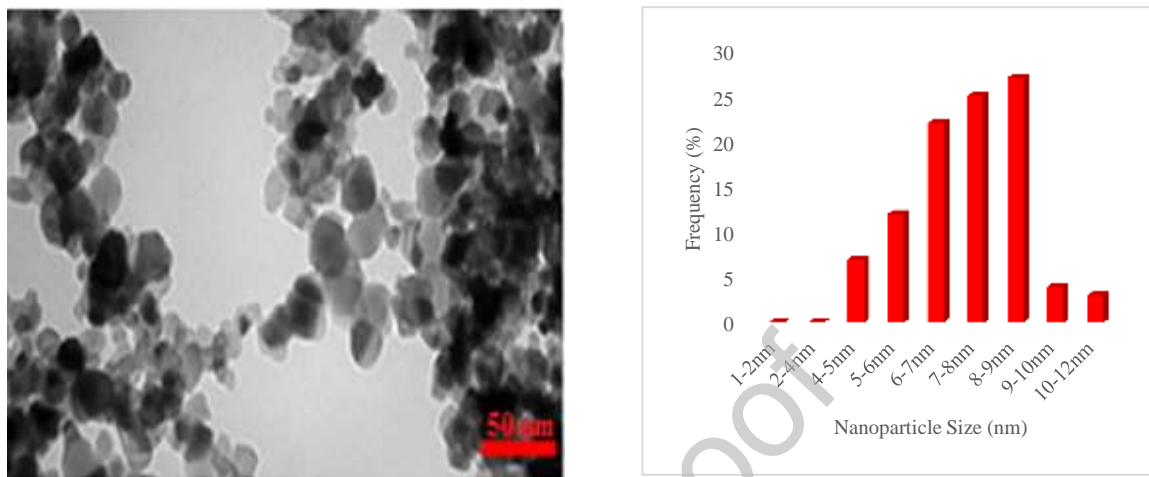


Figure 6. TEM image of nano Ni/g-C₃N₄ (left) showing the distribution of nanoparticle sizes (right).

Also, the result of the BET surface area and pore volumes for nano Ni/g-C₃N₄ measurements is displayed in Table 1. The BET surface area of nano Ni/g-C₃N₄ was detected to be 12.884 m².g⁻¹, and 15.233 m².g⁻¹ represented BJH adsorption surface area of pores. Pore size distribution (7.98 nm) and single point adsorption pore volume of pores (0.1129 cm³.g⁻¹) were distinguished according to Table 1.

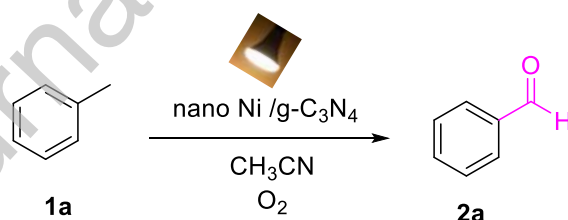
Table 1. Results BET for nano Ni/g-C₃N₄.

| | | |
|--------------|--|--------|
| Surface area | BET surface area (m ² .g ⁻¹) | 12.884 |
| | BJH adsorption cumulative surface area of pores (m ² .g ⁻¹) | 15.233 |
| Pore size | Mean pore diameter (nm) | 35.051 |
| | Pore size distribution (nm) | 7.98 |
| Pore volume | Single point adsorption pore volume of pores (cm ³ .g ⁻¹) | 0.1129 |
| | BJH adsorption cumulative volume of pores (m ² .g ⁻¹) | 0.1147 |
| | | |

3.3. Catalytic application

After the successful preparation of the catalyst, we began our investigation by exposing toluene at visible-light irradiation in the presence of nano Ni/g-C₃N₄. To realize the performance of the catalyst with the various amount of nickel, a set of nano Ni/g-C₃N₄ were prepared with the percentage diverse values of nickel over g-C₃N₄. According to Table 2, it became obvious that nano Ni/g-C₃N₄ with 6 wt% of nickel over the g-C₃N₄ surface is the most effective catalyst, because it was given impressive conversion into 8 h of stirring under 12 W white LED irradiation at room temperature (Table 2, entry 2). Also, the amounts of nano Ni/g-C₃N₄ were optimized, and we were chosen 0.01 g of the catalyst for expediting of the experiment (Table 2, entry 6), because the efficiency of the reaction in the presence of less than 0.01 g of nano Ni/g-C₃N₄ and more than 0.01 g of the catalyst, did not illustrate significant progress on the synthesis of desired products. (Table 2, entries 5, 7). In addition, other accessible photoactive supports such as ZnO and TiO₂, were investigated to afford this reaction under visible light, (Table 2, entries 8 and 9), both of them delivered only <10% of the product, indeed pure ZnO [38, 39] and pure TiO₂ [40, 41] nanoparticles render negligible photocatalytic activity because of their related to high recombination of e⁻/h⁺ transfer and low charge separation proficiency, so they could not absorb the light under the visible light region. In the following (Table 2, entry 10 and 11) neither the g-C₃N₄ nor NiCl₂ alone, were not achieved this transformation. So, it was confirmed that nano Ni/g-C₃N₄ is the best catalyst for this reaction.

Table 2. Optimization conditions:

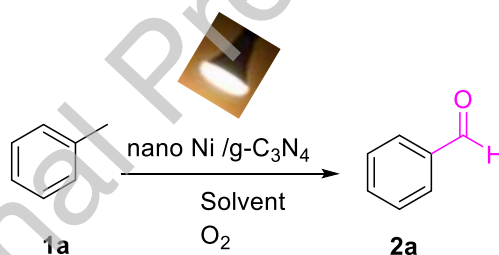


| Entry | Catalyst (wt%, g) | Yield% |
|-----------------|--|--------|
| 1 | Ni/g-C ₃ N ₄ (3, 0.008) | 48 |
| 2 | Ni/g-C ₃ N ₄ (6, 0.008) | 83 |
| 3 ^b | Ni/g-C ₃ N ₄ (9, 0.008) | 68 |
| 4 ^b | Ni/g-C ₃ N ₄ (12, 0.008) | 50 |
| 5 ^b | Ni/g-C ₃ N ₄ (6, 0.006) | 70 |
| 6 ^c | Ni/g-C ₃ N ₄ (6, 0.01) | 95 |
| 7 ^d | Ni/g-C ₃ N ₄ (6, 0.012) | 92 |
| 8 ^e | Ni/ZnO (6, 0.01) | <10 |
| 9 ^e | Ni/TiO ₂ (6, 0.01) | <10 |
| 10 ^f | g-C ₃ N ₄ (0.01g) | <10 |
| 11 ^f | NiCl ₂ (0.01g) | - |

^aReaction conditions: **1a**, (1 mmol), nano Ni/g-C₃N₄, CH₃CN (2 mL), at room temperature, 12 W white LED, isolated product. ^{b,d,f}12 h. ^c8 h. ^eThese catalysts have been prepared according to the literature [42,43], 12h.

According to Tables 3, various solvents and atmospheres were also examined. A series of solvents containing CH₃CN, THF, DMF, 1,4 -Dioxane, EtOAc, CHCl₃, EtOH, H₂O, and solvent-free conditions in the presence of nano Ni/g-C₃N₄ (6 wt%) under white light was checked. As can be shown in Table 3, the outstanding results have been attained with ethanol and acetonitrile (entries 1 and 7). We would rather use EtOH because it is safer and greener than CH₃CN. In terms of atmospheres, almost the same data were obtained for air and O₂. (entries 7, 10). Under an argon atmosphere, there was no favorable product, which demonstrated that the required oxidant in this system is oxygen. (Table 3 entry 11). The effects of light irradiation were also investigated and it was understood that the reaction did not accomplish without light (Table 3, entry 12). This outcome is proof for exciting of nano Ni/g-C₃N₄ by light radiation. Also, the reactions have not proceeded without the use of any photocatalyst. (Tables 3 entry 13).

Table 3. Solvent optimization data^a (C–H Activation)



| Entry | Solvent | Atmosphere | Yield 2a% |
|-----------------|--------------------|----------------|-----------|
| 1 | CH ₃ CN | Air | 95 |
| 2 | THF | Air | 80 |
| 3 | DMF | Air | 75 |
| 4 | 1,4 Dioxane | Air | 90 |
| 5 | EtOAc | Air | 85 |
| 6 | CHCl ₃ | Air | 87 |
| 7 | EtOH | Air | 95 |
| 8 | H ₂ O | Air | 80 |
| 9 | Solvent-free | Air | 65 |
| 10 | EtOH | O ₂ | 98 |
| 11 | EtOH | Argon | 0 |
| 12 ^b | EtOH | O ₂ | 0 |
| 13 ^c | EtOH | O ₂ | 0 |

^aReaction conditions: **1a** (1 mmol), nano Ni/g-C₃N₄ (6wt%, 0.01g), solvent (2 mL), at room temperature, 12 W white LED, 8 h, isolated product. ^bIn dark condition. ^cWithout catalyst after 24 h.

3.4. Influence of light

We investigated the photocatalytic reactions under light irradiation with different wavelengths. Studies have shown the same results were obtained when the reaction mixture was exposed to blue 12 W LED and 12 W white LED irradiation (nano Ni/g-C₃N₄ as photocatalyst and in EtOH), also the selectivity depends on the wavelength when toluene (**1a**) is oxidized by a blue LED irradiation at 400-495 nm, we observed the maximum selectivity, so the blue LED irradiation was selected as a source light. The more effective stimulation of photocatalyst by short wavelengths (higher energy, such as blue) proves the dependence of photocatalytic activity on light-irradiation wavelength. (Figure 7).

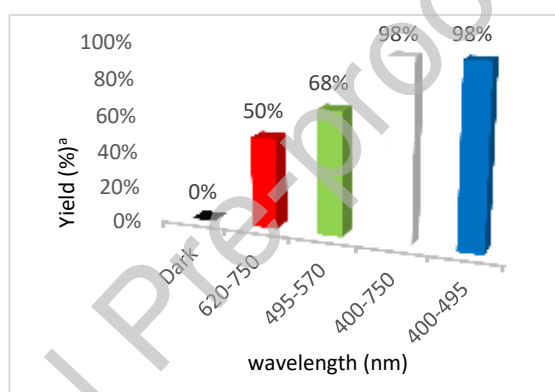


Figure 7. Dependence of the catalytic activity of nano Ni/g-C₃N₄ for C-H activation on the wavelength of the light irradiation. Toluene (1 mmol), nano Ni/g-C₃N₄ (6 wt%, 0.01g), EtOH (2 ml), at room temperature, 8 h. ^aIsolated yield.

3.5. Reaction under sunlight

On a summer day of July in Shiraz city at 68.5° zenith angles with temperature 26-37°C ranges the capability of sunlight nano Ni/g-C₃N₄ was checked in the open air. As can be seen in figure 8, these results indicate the high ability of the photocatalyst under sunlight.

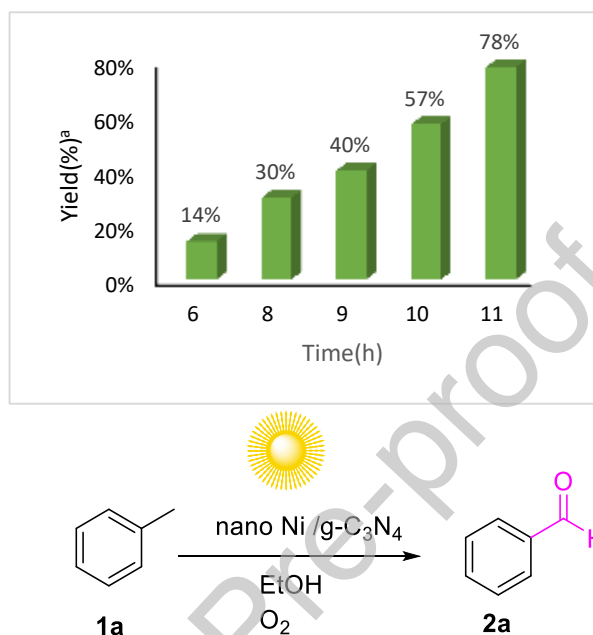
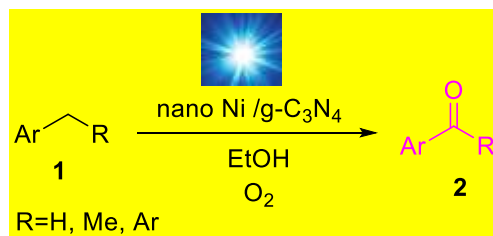


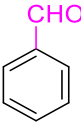
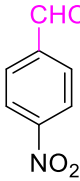
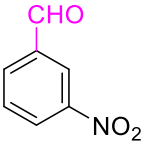
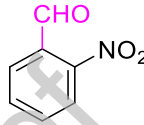
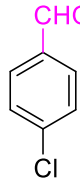
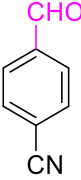
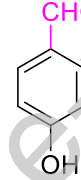
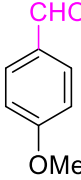
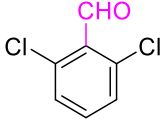
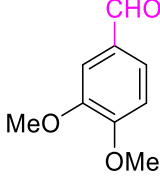
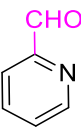
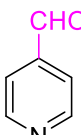
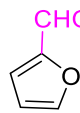
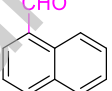
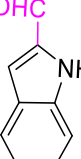
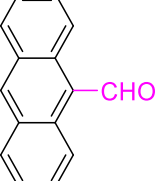
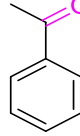
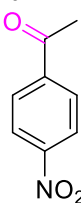
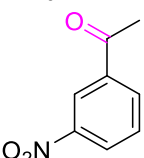
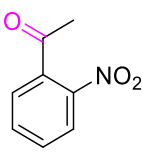
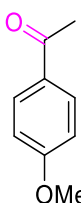
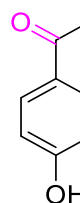
Figure 8. C–H activation under natural sunlight; reaction conditions: Toluene (1 mmol), nano Ni/g-C₃N₄ (6 wt%, 0.01g), EtOH (2 mL), ^aIsolated yield.

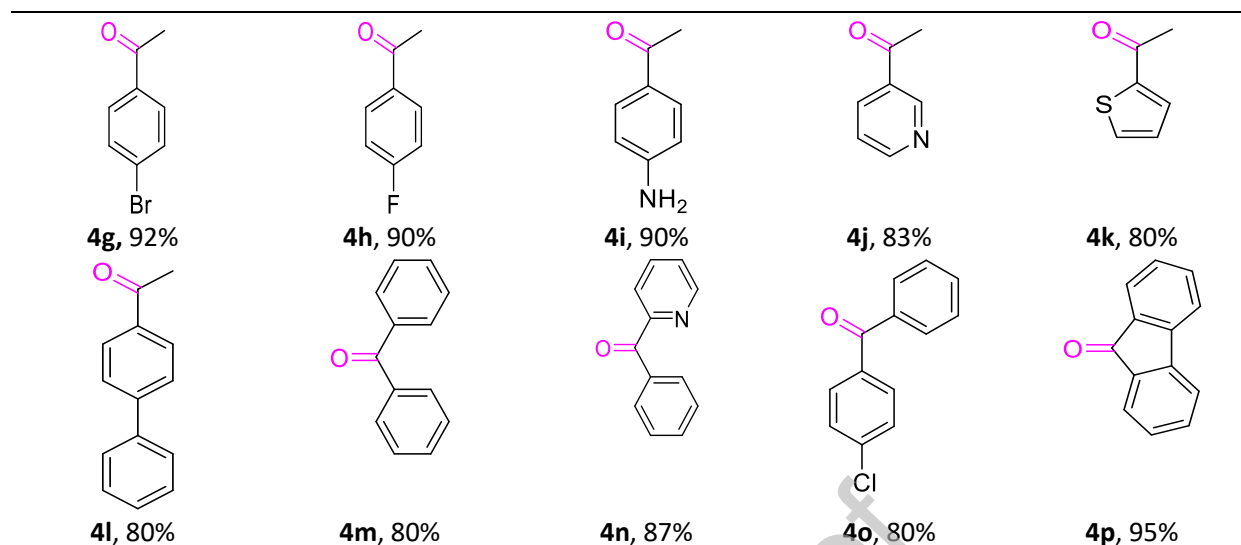
To extend of oxidative C–H activation and study of photocatalytic proficiency, with the optimized conditions obtained a variety of carbonyl compounds have been synthesized. All the reactions were completed at 25 °C under the visible light and condition optimized (ethanol (2 mL) and nano Ni/g-C₃N₄ (6 wt%, 0.01g) as photocatalyst). In the following, the selectivity of these structures for oxidation under heterogeneous conditions in the absence of hydrogen peroxide and the visible-light photocatalytic activity will be described. Different derivatives of methyl arenes were exposed to oxygen by using nano Ni/g-C₃N₄ under visible light (Table 4, entries **2a-2s**); all of the corresponding products were synthesized with good to excellent yields and selectively. The results show that electron withdraw and electron-donating substituents display almost the same effect in reactivity templates. All of the corresponding ketones were prepared via previous conditions in quantitative yields by using substituted methylene arenes. Conforming to observed data, we found that the most appropriate support for prospering of this type of reaction is graphene carbon nitride. As a result, the aromatic system containing a methylene moiety in its

structure (Table 4, entry **4p**) is more reactive in a shorter time (5 h) than the corresponding open-chain substrate (Table 4, entries **4a- 4o**) in time (8 h).

Table 4. Scope of the oxidative (C sp³-H) activation ^{a, b}



| | | | | |
|--|--|--|---|--|
|  2a , 98% |  2b , 95% |  2c , 92% |  2d , 94% |  2e , 90% |
|  2f , 90% |  2g , 87% |  2h , 89% |  2i , 87% |  2j , 85% |
|  2k , 92% |  2l , 95% |  2m , 89% |  2n , 87% |  2o , 92% |
|  2p , 95% |  2q , 89% |  2r , 82% |  2s , 85% |  4a , 98% |
|  4b , 98% |  4c , 98% |  4d , 93% |  4e , 90% |  4f , 94% |



^a Reaction conditions: **1** (1 mmol), nano Ni/g-C₃N₄ (6 wt%, 0.01g), EtOH (2 mL) at room temperature, 12 W blue LED, 8 h. ^b Isolated yield.

This interesting result of the selective oxidation of C-sp³ hydrocarbons causes us to test our system in photo epoxidation of diverse alkenes by utilizing the oxidant agent (air or molecular oxygen) under visible light irradiation at room temperature. In the following, into the epoxidation of alkene substituted, styrene was applied as a model system. Several determinative tests were accomplished to depict different amounts of nickel catalysts, solvent, and atmosphere at ambient temperature. The experimental consequences are represented in Table 5. As evident, the reactivity and activity of the catalysts for the styrene were approximately similar to those obtained from toluene. The only difference was the amount of catalyst and we were chosen 0.012 g of the catalyst for other investigations (Table 5, entry 3). Besides, investigation of the solvent effect in different solvents and solvent-free conditions in the presence of nano Ni/g-C₃N₄ (6 wt%) disclosed the following resultants in the proceeding of the reaction. Yields of products (entries 9-16) were around 50% to 62%. In this manner, acetonitrile was shown the best effect as a solvent (Table 5, entry 3) for epoxidation of styrene. In this reaction, like the C-H activation, oxygen performs an obvious role as the oxidant agent whereas the argon atmosphere does not show promising results (Table 5 entry 18). Also, according to Table 5 entries 19, 20 light absorption and photocatalyst are the major driving force for the reaction because any products were not formed in the absence of them. Besides, toward epoxidation reaction 75% selectivity with 82% conversion was obtained and 7% of styrene was converted to benzaldehyde. (Table 5, entry 17).

Table 5. Selected optimization data ^a

| Entry | Photocatalyst (wt%,g) | Solvent | Atmosphere | Yield 6a | Yield 7a |
|-----------------|---|--------------------|----------------|----------|----------|
| 1 | Ni/g-C ₃ N ₄ (6, 0.008) | CH ₃ CN | Air | 74 | 12 |
| 2 | Ni/g-C ₃ N ₄ (6, 0.01) | CH ₃ CN | Air | 78 | 12 |
| 3 | Ni/g-C ₃ N ₄ (6, 0.012) | CH ₃ CN | Air | 80 | 8 |
| 4 ^b | Ni/g-C ₃ N ₄ (6, 0.014) | CH ₃ CN | Air | 76 | 10 |
| 5 ^b | g-C ₃ N ₄ (0.01g) | CH ₃ CN | Air | trace | 0 |
| 6 ^b | NiCl ₂ (0.01g) | CH ₃ CN | Air | trace | 0 |
| 7 ^c | Ni/ZnO (6, 0.01) | CH ₃ CN | Air | trace | 0 |
| 8 ^c | Ni/TiO ₂ (6, 0.01) | CH ₃ CN | Air | trace | 0 |
| 9 | Ni/g-C ₃ N ₄ (6, 0.012) | THF | Air | 62 | 8 |
| 10 | Ni/g-C ₃ N ₄ (6, 0.012) | DMF | Air | 50 | 16 |
| 11 | Ni/g-C ₃ N ₄ (6, 0.012) | 1,4 Dioxane | Air | 55 | 12 |
| 12 | Ni/g-C ₃ N ₄ (6, 0.012) | EtOAc | Air | 60 | 10 |
| 13 | Ni/g-C ₃ N ₄ (6, 0.012) | CHCl ₃ | Air | 60 | 8 |
| 14 | Ni/g-C ₃ N ₄ (6, 0.012) | EtOH | Air | 53 | 13 |
| 15 | Ni/g-C ₃ N ₄ (6, 0.012) | H ₂ O | Air | 50 | 20 |
| 16 | Ni/g-C ₃ N ₄ (6, 0.012) | Solvent-free | Air | 50 | 23 |
| 17 | Ni/g-C ₃ N ₄ (6, 0.012) | CH ₃ CN | O ₂ | 82 | 7 |
| 18 | Ni/g-C ₃ N ₄ (6, 0.012) | CH ₃ CN | Argon | 0 | 0 |
| 19 ^d | Ni/g-C ₃ N ₄ (6, 0.012) | CH ₃ CN | O ₂ | 0 | Trace |
| 20 ^e | None | CH ₃ CN | O ₂ | 0 | 0 |

^aReaction conditions: 1b (1 mmol), nano Ni/g-C₃N₄ (6 wt%, 0.012 g), solvent (2 ml), at room temperature, 12 W blue LED, 8 h, isolated product. ^{b,c} 12h. ^cThese catalysts have been prepared according to the literature [42,43], ^dIn dark condition. ^e Without catalyst after 24 h.

Likewise, the influence of light and reaction under sunlight is checked and the results are shown in Figure 9. As can be seen from Figure 9a, by using blue 12 W LED the best results were obtained due to the maximum absorption of light by the photocatalyst, however, photons with long wavelengths green (495-570 nm) and red (620-750 nm) cannot transport enough energy to activate the photocatalyst and the epoxidation reaction. Besides in dark conditions, the reaction did not occur. Figure 9b is shown a summer day of August in Shiraz city at 68.5° zenith angles with temperature 28-38 °C ranges and the photocatalytic ability of the nano Ni/g-C₃N₄ under sunlight in the outdoor (Figure 9b).

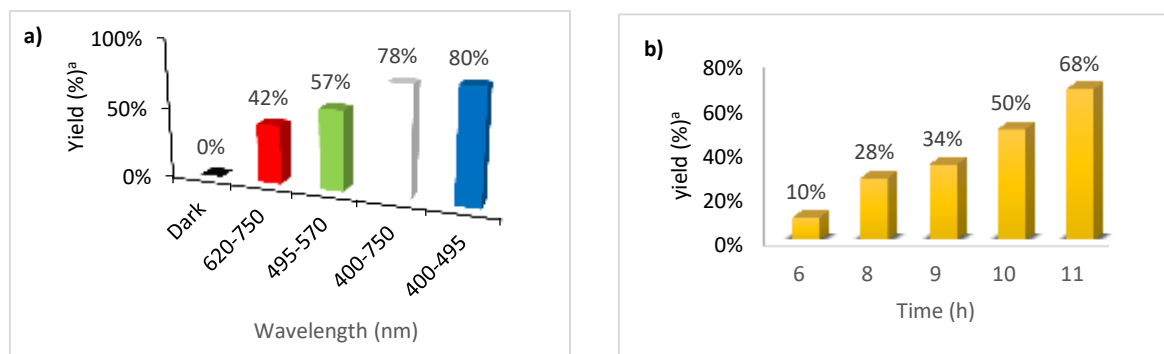
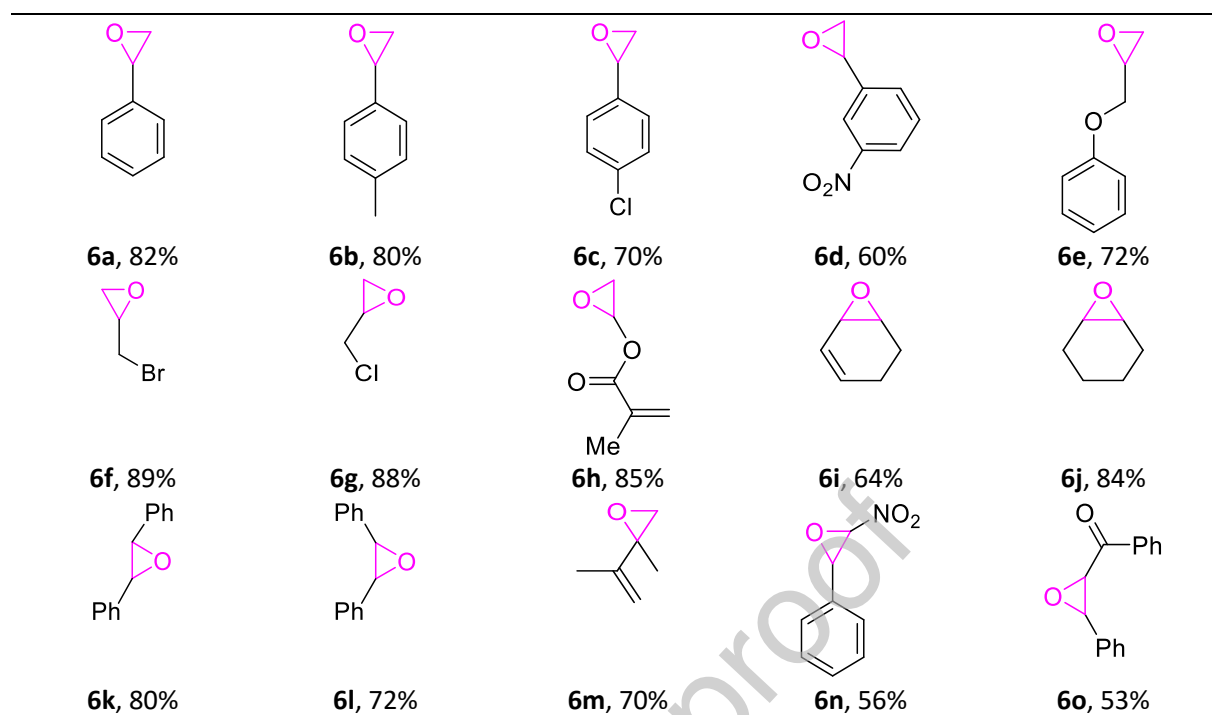


Figure 9. (a) Dependence of the catalytic activity of nano Ni/g-C₃N₄ for epoxidation reaction on the wavelength of the light irradiation, styrene (1 mmol), nano Ni/g-C₃N₄ (6 wt%, 0.012g), CH₃CN (2 ml), at room temperature, 8 h. (b) Epoxidation reactions under natural sunlight; reaction conditions: Styrene (1 mmol), nano Ni/g-C₃N₄ (6 wt%, 0.012 g), CH₃CN (2 mL). ^a Isolated yields.

Subsequently, nano Ni/g-C₃N₄ (6 wt%, 0.012 g) as photocatalyst under blue LED (12 W) irradiation in CH₃CN, at room temperature and under O₂ or air were obtained as the best reaction condition. Some diverse alkenes were assigned to the generalizing of this procedure (Table 6). The results show that for terminal alkenes and cycloalkenes, the epoxidation process was successfully performed with excellent efficiency (Table 6 entries **6a-6j**). Also, the trans-stilbene is more reactive than cis-stilbene (Table 6, entries **6k-6l**). Potent superficial adsorption of π -conjugated molecules onto the Ni metal for reactant with terminal conjugated double bonds (Table 6, entry **6m**), cause Nano Ni/g-C₃N₄ to show worthy implementation. In the case of substrate **5h**, **5i**, & **5m**, no further oxidized products were observed even by increasing the time from 8 hours to 24 hours. Epoxidation of electron-deficient alkenes was shown little activity and lower conversion in comparison with the terminal alkenes (Table 6, entries **6n** and **6o**).

Table 6. Scope of the epoxidation reaction of alkenes ^{a,b}





^aReaction conditions: **5** (1 mmol), nano Ni/g-C₃N₄ (6 wt%, 0.012 g), CH₃CN (2 mL) at room temperature, 12 W blue LED, 8 h, ^b Isolated yield; The yield of products **6f**, **6g**, **6i**, **6j**, **6m** were determined by HPLC analysis.

3.6. Catalyst reusability

The reusability of the nano Ni/g-C₃N₄ photocatalyst was also inquired and the obtained data is exhibited in Figure 10. To recover the photocatalyst, after the accomplishment of each period, it was separated by centrifuging, rinsed with water and ethanol, and then dried at 80°C. In this method, nano Ni/g-C₃N₄ exhibits excellent reusability and any remarkable loss of the catalytic activity was not beholden even after six runs

(Figure 10).

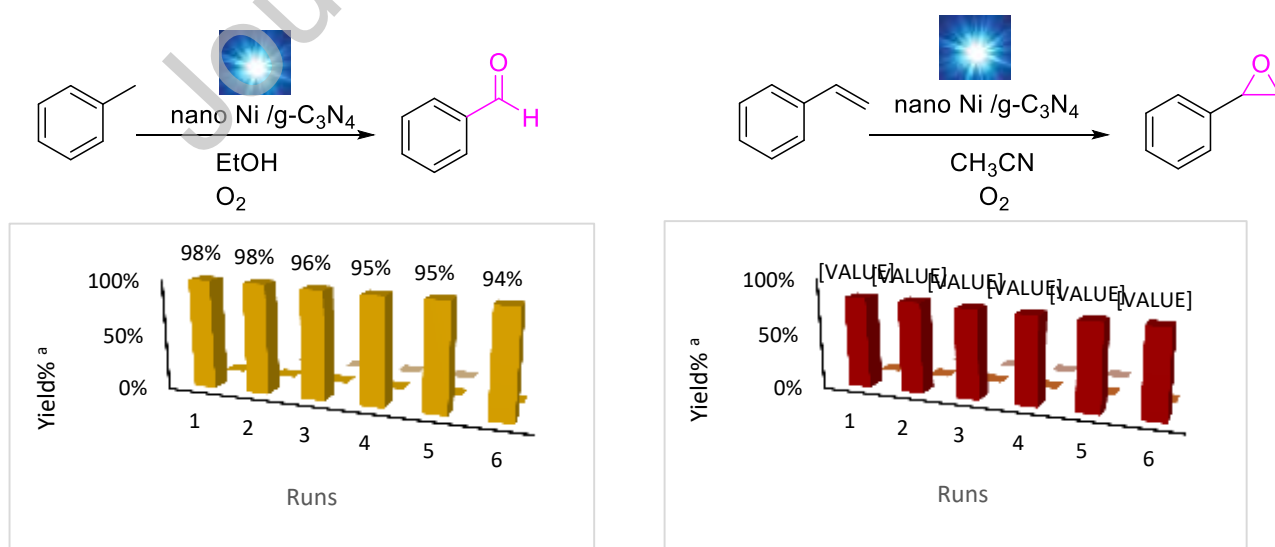


Figure 10. Reusability of the recovered catalyst in C–H activation and epoxidation reactions: Substrate (1 mmol), nano Ni/g-C₃N₄ (6 wt%, 0.012 g), solvent 2 (mL); ^a Isolated yields.

3.7. Leaching test

Details of the weight of the photocatalyst and the wt% of the nickel leaching after each run are given in Tables 7. As can be seen from this table the nano Ni/g-C₃N₄ exhibits excellent reusability and the catalyst sufficiency was not considerably lessened even after 6 sequences. Also, ICP analysis designated the amount of leached nickel. (Tables 7).

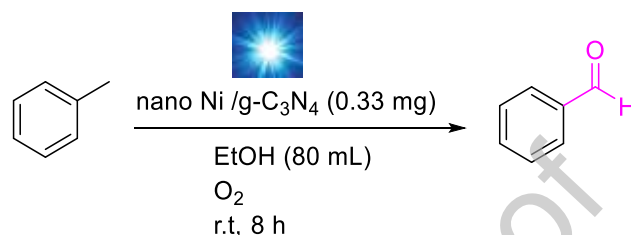
A mixture of toluene (1 mmol), nano Ni/g-C₃N₄ (10 mg, 6wt % Ni), EtOH (2 mL), placed in a glass test tube with a magnetic stirrer bar under 12 W blue LED irradiation (distance 3.0 cm). Similarly, the air atmosphere and room temperature were considered as a reaction condition. The reactant mixture was performed for 8 h. After the accomplishment of time reaction, nano Ni/g-C₃N₄ was separated by centrifuging from the solution and the solvent reaction mixture was used to analyze the Ni content using Inductively Coupled Plasma (ICP) spectroscopy, which indicates that no Ni was detected in the filtrate solution. (Table 7a).

A mixture of styrene (1 mmol), nano Ni/g-C₃N₄ (12 mg, 6wt % Ni), CH₃CN (2 mL), placed in a glass test tube with a magnetic stirrer bar under 12 W blue LED irradiation (distance 3.0 cm). Similarly, the air atmosphere and room temperature were considered as a reaction condition. The reactant mixture was performed for 8 h. After the accomplishment of time reaction, nano Ni/g-C₃N₄ was separated by centrifuging from the solution and the solvent reaction mixture was used to analyze the Ni content using Inductively Coupled Plasma (ICP) spectroscopy, which indicates that no Ni was detected in the filtrate solution. (Table 7b).

Table 7. (a) Catalyst recyclability for C–H activation reaction and (b)Catalyst recyclability for epoxidation reaction.

| Runs (a) | The catalyst weight after each run (mg) | Nickel leaching (wt%) | Runs (b) | The catalyst weight after each run (mg) | Nickel leaching (wt%) |
|----------|---|-----------------------|----------|---|-----------------------|
| 1 | 10 | 0.000 | 1 | 12 | 0.000 |
| 2 | 9.8 | 0.002 | 2 | 11.7 | 0.004 |
| 3 | 9.5 | 0.004 | 3 | 11.4 | 0.007 |
| 4 | 9.1 | 0.007 | 4 | 11 | 0.009 |
| 5 | 8.7 | 0.009 | 5 | 10.7 | 0.012 |
| 6 | 8.4 | 0.011 | 6 | 10.2 | 0.014 |

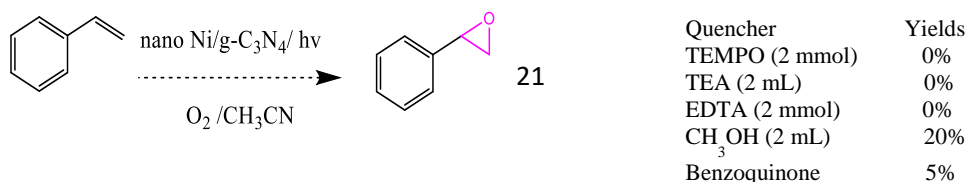
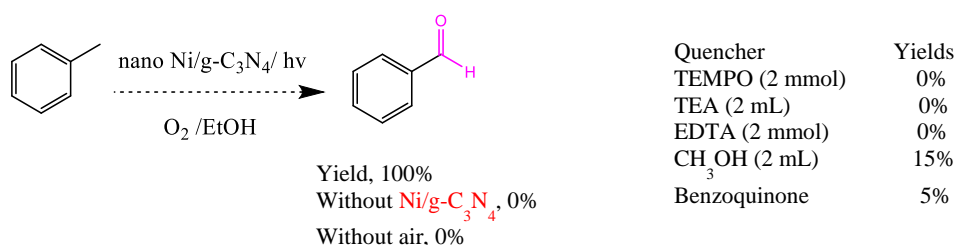
Affordable and recyclable nano Ni/g-C₃N₄, availability of toluene, and no need for any additives cause process scale to be carried out. Satisfactory results using 6.36 mL (60 mmol) of toluene which resulted in 88% benzaldehyde yield (5.60 g). This successful phenomenon suggests that this reaction can be used on a large-scale (scheme 2).



Scheme 2. Gram-scale C–H activation of hydrocarbons.

3.8. Control experiments

A batch of control experiments was run, to figure out the mechanism of the reaction. (Figure 11). When 2 mmol of a radical scavenger such as 2,2,6,6-Tetramethylpiperidiny-1-oxy (TEMPO•), which is a stable nitroxide radical and the electron-trapping standard agent, was added to the reactions system, it could capture electrons, subsequently, the favorable yield of the product in 8h decreased. Also, superoxide radical scavenger (benzoquinone) or hole scavenger (Triethanolamine (TEA), methanol, and ethylenediaminetetraacetic acid) were added. The drastic decrease in the efficiency of the reaction can be a piece of strong evidence that photogenerated hole (h⁺) and superoxide radical anions are the progressive factors for the convert of toluene to benzaldehyde through oxidation reaction and styrene to 2-phenyloxirane (Figure 11).



Yield, 82%
Without Ni/g-C₃N₄, 0%
Without air, 0%

Figure 11. Control experiments

4. Conclusion

As a result, we have demonstrated the first example of a novel and economic ligand-free nano Ni/g-C₃N₄ as photocatalyst under visible light irradiation for C–H activation and epoxidation reaction, with a variety of substrates by using air or O₂ as a green oxygen source and without the use of any reagent or base. Similarly, the reusability of the photocatalyst and the utilization of visible light as attainable energy, are distinctive attributes of this procedure from the eco- friendly viewpoint.

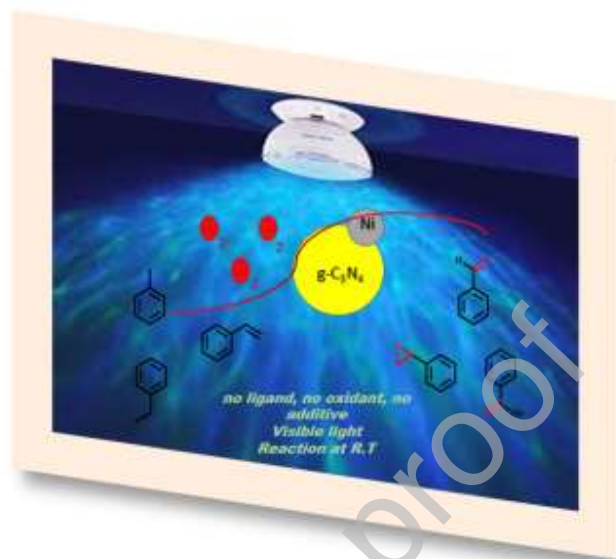
Acknowledgments

This work was supported by Shiraz University Research Council.

Declaration of interests

The authors declare that they have no known competing financial interests or personal relationships that could have appeared to influence the work reported in this paper.

Graphical abstract



References

- [1] M. A. Fox, *Chem. Rev.* 79 (1979) 253-273. <https://doi.org/10.1021/cr60319a002>
- [2] S. J. Jeon, P. J. J. Walsh, *J. Am. Chem. Soc.* 125 (2003) 9544-9545. <https://doi.org/10.1021/ja036302t>
- [3] A. Fingerhut, O. V. Serdyuk, S. B. Tsogoeva, *Green Chem.* 17 (2015) 2042-2058. <https://doi.org/10.1039/C4GC02413C>
- [4] P. Pichat, *Catal. Today.* 19 (1994) 313-333. [https://doi.org/10.1016/0920-5861\(94\)80189-4](https://doi.org/10.1016/0920-5861(94)80189-4)
- [5] J. A. Labinger, J. E. Bercaw, *Nature* 417 (2002) 507-514. <https://doi.org/10.1038/417507a>
- [6] T. Punniyamurthy, S. Velusamy, J. Iqbal, *Chem. Rev.* 105 (2005) 2329-2363. <https://doi.org/10.1021/cr050523v>
- [7] X. Liu, J. Ding, X. Lin, R. H. Gao, Z. H. Li, W. L. Dai, *Appl Catal. A Gen.* 503 (2015) 117-123. <https://doi.org/10.1016/j.apcata.2015.07.010>
- [8] S. Verma, R. B. Nasir Baig, C. Han, M. N. Nadagouda, R. S. Varma, *Chem. Commun.* 51 (2015) 15554-15557. <https://doi.org/10.1039/C5CC05895C>

- [9] S. Verma, R. B. Nasir Baig, C. Han, M. N Nadagouda, R. S. Varma, *Green Chem.* 18 (2016) 251–254. <https://doi.org/10.1039/C5GC02025E>
- [10] F. Rajabi, J. H. Clark, B. Karimi, D. J. Macquarrie, *Org. Biomol. Chem.* 3 (2005) 725–726. <https://doi.org/10.1039/B419322A>
- [11] C. D. Pina, E. Falletta, L. Prati, M. Rossi, *Chem. Soc. Rev.* 37 (2008) 2077–2095. <https://doi.org/10.1039/B707319B>
- [12] Y. Zhang, H. Li, L. Zhang, R. Gao, W. L. Dai, *ACS Sustain. Chem. Eng.* 7 (2019) 17008-17019. <https://doi.org/10.1021/acssuschemeng.9b02683>
- [13] Y. Wang, H. Li, J. Yao, X. Wang, M. Antonietti, *Chem. Sci.* 2 (2011) 446–450. <https://doi.org/10.1039/C0SC00475H>
- [14] M. Jafarpour, F. Feizpour, A. Rezaeifard, *Synlett* 28 (2017) 235–238. <https://doi.org/10.1055/s-0036-1588897>
- [15] Y. Huang, Z. Liu, G. Gao, G. Xiao, A. Du, S. E. Bottle, S. Sarina, H. Zhu, *ACS Catal.* 7 (2017) 4975-4985. <https://doi.org/10.1021/acscatal.7b01180>
- [16] G. Palmisano, V. Augugliaro, M. Pagliaro, L. Palmisano, *Chem. Commun.* 3 (2007) 3425- 3437. <https://doi.org/10.1039/B700395C>
- [17] M. Rueping, J. Zoller, D. C. Fabry, K. Poscharn, R. M. Koenigs, T. E. Weirich, J. Mayer, *Chem. Eur. J.* 18 (2012) 3478-3481. <https://doi.org/10.1002/chem.201103242>
- [18] C. G. Silva, M. J. Sampaio, S. A. C. Carabineiro, J. W. L. Oliveira, D. L. Baptista, R. Bacsá, B. F. Machado, P. Serp, J. L. Figueiredo, A. M.T. Silva, J. L. Faria, *J. Catal.* 316 (2014) 182-190. <https://doi.org/10.1016/j.jcat.2014.05.010>
- [19] B. Chandra, k. k. Singh, S.S. Gupta, *Chem. Sci.* 8 (2017) 7545–7551. <https://doi.org/10.1039/C7SC02780J>
- [20] (a) D. Friedmann, A. Hakki, H. Kim, W. Choi, D. Bahnemann, *Green Chem.* 18 (2016) 5391-5411. <https://doi.org/10.1039/C6GC01582D> (b) S. Samanta, S. Khilari, D. Pradhan, R. Srivastava, *ACS Sustainable Chem. Eng.* 5 (2017) 2562-2577. <https://doi.org/10.1021/acssuschemeng.6b02902> (c) H. Kisch, *Acc. Chem. Res.* 50 (2013) 1002-1010. <https://doi.org/10.1021/acs.accounts.7b00023> (d) W. B. Wu, Y. C. Wong, Z. K. Tan, J. Wu, *Catal. Sci. Technol.* 8 (2018) 4257-4263. <https://doi.org/10.1039/C8CY01240G> (e) K. Kaviyarasu, C. M. Magdalane, D. Jayakumar, Y.

- Samson, A.K.H. Bashir, M. Maaza, D. Letsholathebe, A.H. Mahmoud, J. Kennedy, *J. King Saud. Univ. Sci.* 32 (2020) 1516-1522. <https://doi.org/10.1016/j.jksus.2019.12.006> (f) C. M. Magdalane, K. Kaviyarasu, G. M. A. Priyadharsini, A.K.H. Bashir, N. Mayedwa, N. Mayedwa, N. Matinise, A. B. Isaev, N. A. Al-Dhabi, M. V. Arasu, S. Arokiyaraj, J. Kennedy, M. Maaza, *J. Mater. Sci. Technol.* 8 (2019) 2898-2909. <https://doi.org/10.1016/j.jmrt.2018.11.019> (g) A. Raja, S. Ashokkumar, R. P. Marthandam, J. Jayachandiran, Ch. P. Khatiwada, K. Kaviyarasu, R. G. Raman, M. Swaminathan, *J. Photochem. Photobiol. B.* 181 (2018) 53-58. <https://doi.org/10.1016/j.jphotobiol.2018.02.011> (h) A. Raja, K. Selvakumar, P. Rajasekaran, M. Arunpandian, S. Ashokkumar, K. Kaviyarasu, S. A. Bahadur, M. Swaminathan, *Colloids Surf., A Physicochem. Eng. Asp.* 564 (2019) 23-30. <https://doi.org/10.1016/j.colsurfa.2018.12.024> (i) S. Panimalar, R. Uthrakumar, E. T. Selvi, P. Gomathy, C. Inmozhi, K. Kaviyarasu, J. Kennedy, *Surf. Interfaces* 20 (2020) 100512- 100520. <https://doi.org/10.1016/j.surfin.2020.100512> (j) A. Raja, P. Rajasekaran, K. Selvakumar, M. Arunpandian, K. Kaviyarasu, S. A. Bahadur, M. Swaminathan, *Sep. Purif. Technol.* 233 (2020) 115996- 116006. <https://doi.org/10.1016/j.seppur.2019.115996> (k) A. M. Amanulla, Sk.J. Shahina, R. Sundaram, C. M. Magdalane, K. Kaviyarasu, D. Letsholathebe, S. B. Mohamed, J. Kennedy, M. Maaza, *J. Photochem. Photobiol. B.* 183 (2018) 233-241. <https://doi.org/10.1016/j.jphotobiol.2018.04.034>
- [21] K. Teramura, K. Ogura, T. Sugimoto, H. Tsuneoka, T. Shishido, T. Tanaka, *Chem. Lett.* 38 (2009) 1098-1099. <https://doi.org/10.1246/cl.2009.1098>
- [22] T. S. Symeonidis, A. Athanasoulis, R. Ishii, Y. Uozumi, Y. M. A. Yamada, L. N. Lykakis, *ChemPhotoChem.* 1 (2017) 479-484. <https://doi.org/10.1002/cptc.201700079>
- [23] R. M. Mohameda, M. A. Salam, *Mater. Res.* 50 (2014) 85-90. <https://doi.org/10.1016/j.materresbull.2013.10.031>
- [24] Q. Chen, Y. Xin, X. Zhu, *Electrochim. Acta.* 186 (2015) 34-42. <https://doi.org/10.1016/j.electacta.2015.10.095>
- [25] X. Wang, S. Blechert, M. Antonietti, *ACS Catal.* 2 (2012) 1596-1606. <https://doi.org/10.1021/cs300240x>
- [26] S. Cao, J. Low, J. Yu, M. Jaroniec, *Adv. Mater.* 27 (2015) 2150-2176. <https://doi.org/10.1002/adma.201500033>
- [27] A. Thomas, F. Fischer, M. Goettmann, J. O. Antonietti, R. S. Müller, J. M. Carlsson, *J. Mater. Chem.* 18 (2008) 4893-4908. <https://doi.org/10.1039/B800274F>

- [28] J. Wen, J. Xie, X. Chen, X. Li, *Appl. Surf. Sci.* 391 (2017) 72-123. <https://doi.org/10.1016/j.apsusc.2016.07.030>
- [29] V. W-H Lau, M. B. Mesch, V. Duppel, V. Blum, J. Senker, B. V. Lotsch, *J. Chem. Am. Soc.* 137 (2015) 1064-1072. <https://doi.org/10.1021/ja511802c>
- [30] L. Shen, Z. Xing, J. Zou, Z. Li, X. Wu, Y. Zhang, Q. Zhu, S. Yang, W. Zhou, *Sci. Rep.* 10 (2017) 1038-1048. <https://doi.org/10.1038/srep41978>
- [31] X. Wang, X. Chen, A. Thomas, X. Fu, M. Antonietti, *Adv. Mater.* 21 (2009) 1609–1612. <https://doi.org/10.1002/adma.200802627>
- [32] J. J. Wang, Z. J. Li, X. B. Li, X. B. Fan, Q. Y. Meng, S. Yu, C. B. Li, J. X. Li, C. H. Tung, L. Z. Wu, *ChemSusChem.* 7 (2014) 1468-1475. <https://doi.org/10.1002/cssc.201400028>
- [33] S. C. Yan, Z. S. Li, Z. G. Zou, *Langmuir* 25 (2009) 10397–10401. <https://doi.org/10.1021/la900923z>
- [34] L. Kong, Y. Dong, P. Jiang, G. Wang, H. Zhang, N. Zhao, *J. Mater. Chem. A.* 4 (2016) 9998-10007. <https://doi.org/10.1039/C6TA03178A>
- [35] J. Wen, J. Xie, H. Zhang, A. Zhang, Y. Liu, X. Chen, X. Li, *ACS Appl. Mater. Interfaces.* 9 (2017) 14031-14042. <https://doi.org/10.1021/acsami.7b02701>
- [36] Zh. Jingru, W. Qian, Zh. J. Jiexuan, G. Zhenfei, J.O. L. Zhiwen, L. Shengzhong, *RSC Adv.* 7 (2017) 36722-36727. <https://doi.org/10.1039/C7RA06597C>
- [37] L. Landong, Y. Junqing, W. Tuo, Zh. Zhi-Jian, Zh. Jian, G. Jinlong, G. Naijia, *Nat. Commun.* 6 (2015) 5881-5890. <https://doi.org/10.1038/ncomms6881>
- [38] P. Georgiev, N. Kaneva, A. Bojinova, K. Papazova, K. Mircheva, K. Balashev, *Colloids. Surf. B.* 460 (2014) 240-247. <https://doi.org/10.1016/j.colsurfa.2014.02.004>
- [39] Z. Han, L. Wei, Z. Zhang, X. Zhang, H. Pan, J. Chen, *Plasmonics* 8 (2013) 1193-1202. <https://doi.org/10.1007/s11468-013-9531-0>
- [40] A. K. Tripathi, M. C. Mathpal, P. Kumar, M. K. Singh, S. K. Mishra, R. K. Srivastava, J. S. Chung, G. Verma, M. M. Ahmad, A. Agarwal. *Mater. Sci. Semicond. Process.* 23 (2014) 136-143. <https://doi.org/10.1016/j.mssp.2014.02.041>
- [41] W. Gao, R. dos Reis, L. T. Schelhas, V. L. Pool, M. F. Toney, K. M. Yu, W. Walukiewicz, *Nano Lett.* 16 (2016) 5247- 5254. <https://doi.org/10.1021/acs.nanolett.6b02395>

[42] S. Senapati, S. K. Srivastava, Sh. B. Singh, *Nanoscale* 4 (2012) 6604-6612. <https://doi.org/10.1039/C2NR31831H>

[43] W. T. Chen, A. Chan, D. Sun-Waterhouse, T. Moriga, H. Idriss, G. I. N. Waterhouse, *J. Catal.* 326 (2015) 43-53. <https://doi.org/10.1016/j.jcat.2015.03.008>

Journal Pre-proof